

Probing the *Tetrahymena* Group I Ribozyme Reaction in Both Directions[†]

Katrin Karbstein, Kate S. Carroll, and Daniel Herschlag*

Department of Biochemistry, Stanford University, Beckman Center B400, Stanford, California 94305-5307

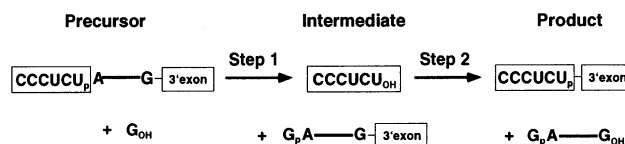
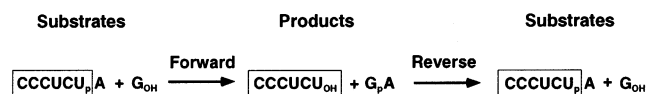
Received April 5, 2002

ABSTRACT: The *Tetrahymena* L-21 *ScaI* ribozyme derived from the self-splicing group I intron catalyzes a reversible reaction analogous to the first step of self-splicing: CCCUCUA (S) + [UC]G \rightleftharpoons CCCUCU (P) + [UC]GA. To relate our understanding of the ribozyme to the self-splicing reaction and to further the mechanistic dissection of the ribozyme reaction, we have established a quantitative kinetic and thermodynamic framework for the forward and reverse reaction of the L-21 *ScaI* ribozyme under identical conditions. Examination of the framework shows that binding of products is cooperative with binding enhanced 5-fold, as was observed previously for binding of the substrates. Further, binding of UCGA is 12-fold weaker than binding of the unphosphorylated UCG, analogous to the 20-fold weaker binding of phosphorylated S relative to P; the molecular interactions underlying the stronger binding of UCG were traced to the 3'-hydroxyl group of UCG. The symmetrical effects on binding of substrates and products result in the equilibrium between ribozyme-bound species, K_{int} , that is essentially unperturbed from the solution equilibrium, K_{ext} ($K_{\text{int}} = [\text{E}\cdot\text{P}\cdot\text{UCGA}]/[\text{E}\cdot\text{S}\cdot\text{UCG}] = 4.6$ and $K_{\text{ext}} = [\text{P}][\text{UCGA}]/[\text{S}][\text{UCG}] = 1.9$). Last, we show that the $\text{p}K_{\text{a}}$ values of the nucleophiles in the forward and reverse reactions are ≥ 10 . This observation suggests that metal ion activation of the nucleophile and stabilization of the leaving group can only account for a portion of the rate enhancement of this ribozyme. These and prior results suggest that the *Tetrahymena* group I ribozyme, analogous to protein enzymes, uses multiple catalytic strategies to achieve its large rate enhancement.

To broadly and deeply understand the behavior and function of RNA, the *Tetrahymena* group I intron has served as a versatile and powerful model system (e.g., refs 1, 3, 6, and 9–16). Most studied has been the reaction of a ribozyme derived from the self-splicing intron, the L-21 *ScaI* ribozyme. This ribozyme catalyzes a transesterification reaction analogous to the first step of self-splicing (Scheme 1). The ribozyme binds an exogenous guanosine (G), which serves as the nucleophile to attack a 5'-splice site analogue (CCCUCU_PA) to yield G_PA and a 5'-exon analogue (CCCUCU). A kinetic and thermodynamic characterization of the forward reaction has provided the basis for mechanistic studies: additional reaction steps have been discovered, a detailed picture of catalytic interactions has been established, features of the reaction, such as strong binding of the 5'-exon, have been related to the intron's biological role in self-splicing, and energetic principles of biological catalysis have emerged (e.g., refs 3, 6, 10, 12, 13, and 17–21).

The majority of studies of catalysis by the *Tetrahymena* ribozyme have focused on the forward reaction, in part because it mimics the first step in self-splicing and in part because the reverse reaction has been more difficult to dissect in detail. Nevertheless, study of the reverse reaction is of interest as it mimics the second step in self-splicing (Scheme 1), and development of a quantitative framework for the reverse reaction would further our basic understanding of

Scheme 1

A: Self-splicing**B: Ribozyme Reaction**

this RNA enzyme. Different aspects of the reverse reaction have been studied in different laboratories, with different ribozyme constructs and different substrates and under different reaction conditions (21–26). The experimental variations limit the ability to compare these studies and to integrate the findings with information about the forward reaction.

In this work, we have used information garnered from these and other kinetic and thermodynamic studies to establish conditions to quantitatively probe the reverse reaction. Because there is added power in determining a complete reaction profile and in comparing the binding and behavior of substrates and products (e.g., refs 27–32), we have also reinvestigated the forward reaction under the conditions amenable to study of the reverse reaction. Thus, an overall framework for the reaction in both directions has

[†] This work was supported by NIH Grant GM49243. K.K. was supported by a fellowship from the Boehringer Ingelheim Foundation.

* To whom correspondence should be addressed. Phone: 650-723-9442. Fax: 650-723-6783. E-mail: herschla@cmgm.stanford.edu.

Chart 1^a

| Abbreviation | Oligonucleotide | Attributes |
|-------------------------------|--------------------------------------|-----------------------------|
| 5'-Splice-site Analogs | | |
| | Position: -3 -1 +1 | |
| rSA | rC rC rC rU rC rU rA | Wild type |
| -1d,rSA | rC rC rC rU rC dT rA | Slower chemical step |
| -3m,rSA | rC rC rC mU rC rU rA | Undocked |
| dSA ₅ | dC dC dC dT dC dT dA dA ₄ | Weak binding, slow reaction |
| -1r,dSA ₅ | dC dC dC dT dC rU dA dA ₄ | Weak binding, fast reaction |
| 5'-Exon Analogs | | |
| | Position: -3 -1 | |
| rP | rC rC rC rU rC rU | Wild type |
| -1d,rP | rC rC rC rU rC dT | Slower chemical step |
| -1d, ^Δ P | rC rC rU rC dT | Faster dissociation |
| -1r,dP | dC dC dC dT dC rU | Weak binding, fast reaction |
| dP | dC dC dC dT dC dT | Weak binding, slow reaction |

^a r = 2'-OH; d = 2'-H, m = 2'-OCH₃.

been established, and new insights into active site interactions have been obtained.

MATERIALS AND METHODS

Materials. Ribozyme was prepared by in vitro transcription with T7 RNA polymerase and purified using Qiagen RNeasy columns as described previously (33, 34). RNA oligonucleotides were purchased from Dharmacon Research, Inc. (Lafayette, CO), or the Protein and Nucleic Acids Facility at Stanford, and DNA oligonucleotides were purchased from Operon Technologies Inc. (Alameda, CA). RNA and DNA oligonucleotides were 5'-end-labeled with [γ -³²P]ATP and gel purified using standard procedures (33). 3'-Deoxyguanosine (3'dG)¹ was purchased from Sigma; analytical HPLC showed $\leq 0.5\%$ contamination by guanosine.

Chart 1 lists the oligonucleotides used in this study. UCG and UCGA were purified by anion-exchange HPLC and desalted on Sep-Pak C-18 columns (Waters, Franklin, MA).

General Kinetic Methods. All reactions were single turnover with ribozyme in excess of 5'-³²P-labeled S or P and, unless otherwise noted, were carried out at 30 °C in 50 mM Na-MES, pH 6.0, and 10 mM MgCl₂. Prior to reaction, ribozyme was preincubated for 30 min at 50 °C and pH 6.0

¹ Abbreviations: S, the 5'-splice site analogue without specifying the identity of the 2'-substituents, which can be hydrogen atoms or hydroxyl or methoxy groups (the length of the "tail" 3' of the cleavage site is also not specified) (see Chart 1 for the specific oligonucleotides used); P, the 5'-exon analogue (see Chart 1) without specifying the identity of the 2'-substituents as for S; E, L-21 *Scal* ribozyme; MES, 2-(*N*-morpholino)ethanesulfonic acid; MOPS, 3-(*N*-morpholino)propanesulfonic acid; EPPS, 4-(2-hydroxyethyl)piperazine-1-propanesulfonic acid; CHES, 2-(*N*-cyclohexylamino)ethanesulfonic acid; HEPES, 4-(2-hydroxyethyl)piperazine-1-ethanesulfonic acid; EDTA, ethylenediaminetetraacetic acid; $K_{1/2}$, the concentration at which the half-maximal rate constant is observed; G, guanosine; 3'dG, 3'-deoxyribo-guanosine; 3'dP, CCCUCU product analogue with a 3'-deoxyribose substitution at U(-1).

with 10 mM MgCl₂ to allow folding to the active state (6, 35). Reaction aliquots were quenched using 2 volumes of a solution containing 20 mM EDTA and 85% formamide. Radiolabeled oligonucleotides were separated by denaturing gel electrophoresis (7 M urea, 20% acrylamide) and quantitated using Phosphorimager analysis (Molecular Dynamics) with Image Quant quantitation software. For slow reactions, rate constants were obtained from initial rates assuming end points of 90%. All other reactions were followed to completion, and good first-order fits to the data with end points of $\geq 90\%$ were obtained ($R^2 \geq 0.98$) (Kaleidagraph, Synergy Software, Reading, PA).

Association and Dissociation Rate Constants for the 5'-Splice Site Analogue (S) and 5'-Exon Analogue (P). Dissociation and association rate constants for S and P were determined with rSA or rP (Chart 1), unless otherwise noted. Figure 2A defines the rate constants (k_1 through k_{-8}) referred to throughout the text.

Dissociation rate constants for the 5'-exon analogue (P) from the E•P complex (k_{-7}) were determined in pulse-chase experiments, as previously described (6). In these reactions, the radiolabeled 5'-exon analogue (*P) was added to saturating amounts of folded ribozyme ("pulse"; 50–500 μ M E; $K_d = 15$ pM). After a short time t_1 , sufficient for essentially complete binding of *P, the dissociation reaction was initiated by the addition of a large excess (≥ 10 -fold over ribozyme) of unlabeled P ("chase") to prevent rebinding of dissociated *P. Control reactions confirmed that the chase was effective in preventing rebinding of *P. After waiting for specified times t_2 UCGA was added to allow fast reaction of *P that remained bound. Because the chemical step occurs much faster than dissociation of P (see Results), the fraction of *P that remained bound during the chase equals the fraction of reacted *P (after a small correction for the fraction of active molecules). The fraction of bound *P was plotted against t_2 and fit to an exponential decay (eq 1) to yield the dissociation rate constant k_{-7} .

$$\text{frac}_{\text{bound}} = \text{frac}_{\text{bound}}^{t_2=0} \exp(-k_{-7}t_2) \quad (1)$$

The dissociation rate constants for P, for a 5'-shortened form, Δ P (Chart 1), and for -1d,rSA from E•P (k_{-7}), E• Δ P (k_{-7}), and E•S (k_{-1}), respectively, were obtained independently in pulse-chase gel-shift experiments (21). -1d,rP and -1d,rSA (Chart 1) were used to allow more direct comparison with the experiments in which UCG or UCGA were also present. Trace *P (or * Δ P or *S) was bound to saturating amounts of ribozyme, and a large excess of unlabeled P was then added. At specified times aliquots were loaded onto a running native gel in THEM buffer (33 mM Tris, 67 mM HEPES, 1 mM EDTA, 10 mM MgCl₂). Dissociation rate constants of -1d,rP obtained from pulse-chase gel-shift and cleavage experiments agreed within error (20%).

The dissociation rate constants of -1d,rSA from E•S•UCG (k_{-4}) and of -1d,rP from E•P•UCGA (k_{-8}) were obtained from experiments that measured the partitioning of molecules in the E•S•UCG complex between dissociation of S (k_{-4}) and reaction of the ternary complex (k_5) [or partitioning of E•P•UCGA between dissociation of P (k_{-8}) and reaction (k_{-5})]. To accurately determine the rate constant for dissociation in these experiments, the values of k_{-4} and k_5 (or k_{-8} and k_{-5}) must be similar. To accomplish this for the

dissociation of P, a 5'-exon analogue shortened by one residue at its 5'-end to give CCUCdT (Δ P) was used. Previous results have shown that removing the 5'-most residue of P weakens binding via base pairing with the ribozyme but does not significantly affect docking of the ribozyme–substrate duplex into the active site or the subsequent chemical step (36, 37). Shortening P at the 5'-end was therefore used to modulate its affinity without affecting other reaction steps. This was necessary for P but not for S because P docks more strongly into the active site than S (12), resulting in slower dissociation of P than S.

To determine the partitioning, radiolabeled *S (or Δ P) was bound to the ribozyme (100 nM) to allow for formation of E·*S (or E· Δ P). Reaction was initiated by addition of UCG ([UCG] = 100 μ M; $K_d^{\text{UCG}} = 7 \mu$ M) (or UCGA: [UCGA] = 950 μ M, $K_d^{\text{UCGA}} = 88 \mu$ M) to rapidly form the E·*S·UCG (or E· Δ P·UCGA) complex, along with a large excess (1 μ M) of unlabeled P to prevent rebinding of dissociated *S (or Δ P). The observed rate constant for formation of *P from *S (or *S from *P) is the sum of the rate constants for the chemical step and dissociation of S (or P) from the ternary complex. Thus, by independently measuring the rate constant for the chemical step in reactions with the chase omitted (k_5 or k_{-5}), one can calculate the dissociation constant according to eq 2A (for S). Alterna-

$$k_{-4} = k_{\text{obs}} - k_5 \quad (2A)$$

$$\text{frac}_{\text{reacted}} = \frac{k_5}{k_5 + k_{-4}} \quad (2B)$$

tively, the dissociation rate constant can be obtained from the fraction of *S (or Δ P) that reacted, relative to reactions in which no chase was added, and the rate constant of the reaction in the presence of the chase (eq 2B). The dissociation rate constants obtained from these two methods were the same within 10%.

The observed dissociation rate constant $k_{-4,\text{obs}}$ is a weighted average of the dissociation rate constants for S from E·S, k_{-1} , and from E·S·UCG, k_{-4} (eq 3A). Analogously, $k_{-8,\text{obs}}$

$$k_{-4,\text{obs}} = k_{-4}(\text{fraction}_{\text{E}\cdot\text{S}\cdot\text{UCG}}) + k_{-1}(\text{fraction}_{\text{E}\cdot\text{S}}) \quad (3A)$$

$$K_{d,\text{obs}}^{\text{UCGA}} = K_d^{\text{UCGA}}(\text{fraction}_{\text{E}\cdot\text{P}}) + K_d^{\text{UCGA}}(\text{fraction}_{\text{E}}) \quad (3B)$$

is the weighted average of the dissociation rate constants of Δ P from E· Δ P, k_{-7} , and E· Δ P·UCGA, k_{-8} . To account for the small fraction of E·S that has no UCG bound (or fraction of E· Δ P without UCGA), the measured dissociation rate constants were extrapolated to the rate constant with UCG fully bound using eq 3A and the measured equilibrium dissociation constants for UCG (and UCGA).

Association rate constants for rSA (or rP) in the presence (k_4 or k_8) and absence (k_1 or k_7) of UCG or UCGA were determined side by side from reactivity measurements. In these experiments the observed first-order rate constant was measured at several subsaturating ribozyme concentrations (4–12 nM) in the presence of saturating concentrations of UCG (k_4) and subsaturating concentrations of G (k_1) for rSA or saturating (k_8) and subsaturating (k_7) concentrations of UCGA for rP (200 μ M UCG, $K_d^{\text{UCG}} = 36 \mu$ M; 50 μ M G, $K_d^{\text{G}} = 400 \mu$ M; 990 or 50 μ M UCGA, $K_d^{\text{UCGA}} = 450 \mu$ M).

[Note that these ribozyme concentrations that are greater than the dissociation constant for E·rSA and E·rP complexes are nevertheless subsaturating, as the rate constant for reaction of the bound oligonucleotide is faster than dissociation under these conditions (6, 36, 37; Figure 2B).] Plots of the observed first-order rate constants against ribozyme concentration were linear in all cases ($R^2 \geq 0.96$) and gave the association rate constants reported in Figure 2B.

Measurement of UCG and UCGA Affinities. To determine the affinities for UCG (or UCGA) to ribozyme complexes with or without bound *S or *P, the rate of reaction of *S (or *P) was determined with varying concentrations of UCG (0–400 μ M) (or UCGA, 10–2000 μ M). This observed rate constant was plotted as a function of UCG (or UCGA) concentration and fit by eq 4. The following suggests that

$$k_{\text{obs}} = \frac{k_{\text{max}}[\text{UCG}]}{[\text{UCG}] + K_{1/2}^{\text{UCG}}} \quad (4)$$

the observed $K_{1/2}$ values equal the dissociation constants K_d (see also ref 37): The same $K_{1/2}$ values were observed in concentration dependences in which the maximal rate constant for reaction varied by more than 10-fold, which was accomplished by a 2'-H substitution at position -1 and by varying the pH (38).

The affinity of S or P for the ribozyme is very high (see Figure 2B and Results), such that nonspecific losses to the tube walls are observed at the low ribozyme concentrations at which S or P will not be bound (<1 nM). To avoid these losses, ribozyme concentrations ≥ 2 nM were used in all experiments. This meant, however, that S and P were bound to the ribozyme under all equilibrium conditions. To obtain the affinity of UCG to free ribozyme, we made use of the observation that S binds to the ribozyme in two steps: base pairing to form a duplex between S and the ribozyme, followed by docking of the duplex into the active site (e.g., refs 10, 17, 39, 40). 5'-Splice site analogues that cannot dock stably into the active site (-3m,rSA₅, dSA₅, Chart 1) are therefore bound only through base pairing interactions and are located away from the active site. These “undocked” 5'-splice site analogues can therefore be used to model interactions with the free ribozyme (1, 39). In contrast, neither the -3-methoxyribose nor all-deoxyribose substitutions destabilized docking sufficiently to undock P (data not shown), as P is docked more strongly than S (12 and Figure 2B). Therefore, the strategy of using undocked P for measurements to free ribozyme could not be used. Instead, control experiments in which the concentration of ribozyme was varied between 50 and 600 nM suggested that dP binds with a K_d of ≈ 150 nM (data not shown). Thus, experiments with dP could be carried out with 50 nM ribozyme, a concentration that leaves dP mostly unbound. To account for the fraction of product that remained bound at 50 nM ribozyme, the observed K_d was extrapolated to a K_d in which no dP was present using eq 3B and $K_d^{\text{dP}} = 150$ nM.

Measurement of Rate Constants for the Chemical Step. The rate constants for the forward and reverse chemical step (k_5 and k_{-5}) were measured by forming E·S·UCG (or E·P·UCGA) and following the formation of P (or S). The ribozyme concentration was 710 nM, with 100 μ M UCG ($K_d = 7 \mu$ M) or 675 μ M UCGA ($K_d = 88 \mu$ M). The observed

pH dependence in both directions suggests that the chemical step is rate-limiting in these experiments (data not shown; 41, 42). The wild-type 5'-splice site analogue rSA and the wild-type 5'-exon analogue rP were used in these experiments. To follow the rates of reaction of these unmodified oligonucleotides by manual pipetting, reactions were performed at pH 5.7–7.2.

Internal and External Equilibria. The internal equilibrium constant, K_{int} (eq 5A), was calculated from the rate constants for reaction of the ternary complexes of bound substrates and products, k_5 and k_{-5} , which describe the forward and reverse reactions, respectively (eq 5B). These rate constants were determined side by side as described in Measurement of the Rates of the Chemical Step. The value of K_{int} determined independently from the extent of reaction agreed within 20% (data not shown).



$$K_{\text{int}} = \frac{[E \cdot P \cdot UCGA]}{[E \cdot S \cdot UCG]} = \frac{k_5}{k_{-5}} \quad (5B)$$

The external equilibrium constant K_{ext} describes the equilibrium between free substrates and free products (eq 6A). The standard 5'-exon analogue binds with a dissociation constant of 15 pM (Figure 2B), and with ribozyme concentrations this low the ribozyme-catalyzed reaction is too slow relative to background RNA hydrolysis to allow equilibration. We therefore used an alternative pair of 5'-splice site and 5'-exon analogues, $-1r,dSA_5$ and $-1r,dP$, which bind less strongly ($K_d = 85$ and ~ 150 nM for $-1r,dSA_5$ and dP , respectively; ref 43 and data not shown). We then used a series of analogues to relate this equilibrium to that for the all-RNA analogues, as described below. Reactions were



$$K_{\text{ext}} = \frac{[E][P][UCGA]}{[E][S][UCG]} \quad (6B)$$

$$\text{frac}_p = \frac{K_{\text{ext}}}{K_{\text{ext}} + [UCGA]/[UCG]} \quad (6C)$$

carried out with 20–50 nM E, 1–5 μM UCG, and 5–40 μM UCGdA₅. *S or *P was used in trace so UCG and UCGdA₅ concentrations were essentially unchanged throughout the course of the reaction. The value of K_{ext} was calculated from the fraction of *P formed from *S at different ratios of UCGdA₅/UCG according to eq 6C, which was derived from eq 6B. Control experiments in which the ribozyme concentration or the concentrations of UCG and UCGdA₅ were varied while maintaining a constant ratio [UCGdA₅]/[UCG] gave faster reaction but no change in the observed extent of reaction, indicating that substrates and products were subsaturating. The same value of K_{ext} , within 15%, was obtained from reactions initiated with *P.

As noted above, the external equilibrium constants were obtained using 5'-splice site analogues that differ from the oligonucleotides used to obtain the internal equilibrium constant having deoxyribose residues and a longer "tail" 3' to the splice site [d(CCCCTC)rUdA₅ vs r(CCCUCUA)]. To

test whether these differences influence the equilibrium, we determined the value of K_{ext} with a dA₅ tail and an A tail [d(CCCCTC)rUdA₅ vs d(CCCCTC)rUrA]. The same value for K_{ext} was obtained in both cases (within 20%). This suggests that the length and the sugar identity of the A-tail do not influence the equilibrium K_{ext} . Furthermore, we also found that the internal equilibrium constant K_{int} is not affected by the length of the A-tail [r(CCCUCUA) vs r(CCCUCUA₅)] (within 30%). Last, high temperature destabilizes binding of the rSA substrate sufficiently such that the external equilibrium can be measured with this substrate. Using rSA at 60 °C the same value for K_{ext} was obtained as for $-1r,dSA_5$ at 30 °C ($K_{\text{ext}} = 1.7$ and 1.9, respectively). These results strongly suggest that the differences between these substrates away from the scissile bond do not influence the equilibrium constants K_{int} and K_{ext} .

Measurement of the Affinity for 3'dG. 3'dG does not have measurable activity in the ribozyme reaction (44, 45; data not shown). We therefore determined its affinity by competitive inhibition (eq 7) with a subsaturating concentration of guanosine (50 μM G, $K_d^G = 400$ and 970 μM at 10 and 2 mM Mg²⁺, respectively; Table 2). Experiments were carried out in 50 mM Na-MOPS, pH 7.7, with 0–4.6 mM 3'dG, using $-3m,rSA_5$ in the presence of 2 mM MgCl₂ or 10 mM MgCl₂. The $-3m,rSA_5$ substrate and the low metal ion concentration were used to ensure that neither S nor metal ion B was bound at the active site. The observed rate constant for reaction of *S exhibited only a small decrease in rate (35%) at the highest 3'dG concentration attainable so only a lower limit for the dissociation constant could be determined.

$$k_{\text{obs}} = \frac{k_{\text{max}}K_d^{3'dG}}{K_d^{3'dG} + [3'dG]} \quad (7)$$

Probing the pK_a of the 3'-OH of G. To determine the pK_a for the 3'-OH of the attacking guanosine nucleophile, the rate constant for the chemical step, k_5 , was measured over a wide range of pH values. To ensure that the chemical step was slower than binding and conformational steps and to stabilize the active ribozyme, experiments were performed at 4 °C using the $-1d,rSA_5$ substrate. In addition, 100 mM MgCl₂ was used to stabilize the active ribozyme at high pH values and to fully saturate metal ion B [$K_d \sim 6$ mM at 30 °C (1)]. Experiments were carried out using 50 nM E and 2 mM G. Control experiments showed no pH dependence of the K_d^G between pH 6.5 and pH 9.0. The following buffers were used: sodium acetate, pH 4.5–5.5, Na-MES, pH 5.4–6.7, Na-MOPS, pH 6.5–7.9, Na-EPPS, pH 7.9–8.6, and Na-CHES, pH 8.6–10.1. pH values were measured at 25 °C, and no temperature correction was made to 4 °C. Prior control experiments revealed no buffer-specific effects under analogous conditions (41). The pH dependence of the observed rate constants was fit to eq 8.

$$k_{\text{obs}} = \frac{k_{\text{max}}}{1 + 10^{pK_a - \text{pH}}} \quad (8)$$

Probing the pK_a of the 3'-OH on U(-1). To determine the pK_a for the 3'-OH on U(-1), the rate constant of the reverse reaction was followed as a function of pH at 30 °C. The same buffers were used as for probing the pK_a of the

3'-OH of G. Experiments were performed at 20 mM MgCl₂ to saturate the catalytic metal ion sites (1).

To determine the pK_a for the 3'-OH on U(-1), it was necessary to use the fast-reacting 5'-exon analogue rP instead of -1d,rP. This is because substituting the 2'-OH at U(-1) increases the pK_a of the 3'-OH at that residue, making it more difficult to observe deprotonation over an experimentally accessible range (4).

At high pH values, the reverse reaction was observed to be biphasic (Figure S1, Supporting Information). In the burst phase the internal equilibrium is established, whereas the reaction is rendered irreversible by the dissociation of UCG in the second kinetic phase (unpublished results). Thus, to probe the pH dependence of the chemical step, the burst phase was followed. To ensure the accuracy of the rate measurements, it was necessary to use a quench-flow apparatus (KinTek Corp., Austin, TX). In these experiments, preformed E•*P (400 nM E•P) was loaded in syringe A, GUCGA (400 μM, K_d = 42 μM) at the desired pH was loaded in syringe B, and syringe C contained stop solution. GUCGA was used instead of UCGA to reduce the amounts of materials used, as GUCGA binds more strongly than UCGA (34; data not shown) and as large volumes were used in these experiments.

The pH maximum of these experiments was determined by the highest concentration of GUCGA that could be used in practice (400 μM). At pH values above ~8.0 the chemical step became faster than binding of GUCGA, so that the chemical step was no longer directly followed (unpublished results). Nevertheless, information about the pH dependence of the reverse chemical step (*k*₋₅) can be obtained from the size of the burst combined with knowledge about the pH dependence for the rate constant for the forward chemical step according to eq 9. For example, increasing the forward rate constant *k*₅ without accelerating the reverse rate constant *k*₋₅ would decrease frac_{fast}. Conversely, a constant frac_{fast} over a range of pH values would indicate the same pH dependence for the forward and reverse reaction.

$$\text{frac}_{\text{fast}} = \frac{k_{-5}}{k_{-5} + k_5} \quad (9)$$

RESULTS

We first describe the framework for the *Tetrahymena* L-21 *ScaI* ribozyme reaction in the forward and reverse reaction. To enhance our understanding of active site interactions of substrates and products, the binding affinities for analogues with single atom substitutions were measured and compared to the affinities for substrates and products. Last, we further dissect the central part of the reaction, including conversion between bound substrates and products, to probe the protonation state of the bound nucleophile in each reaction direction.

Framework for the Ribozyme Reaction. As described in the introduction, the forward reaction catalyzed by the *Tetrahymena* ribozyme has been well studied. Characterization of the reverse reaction has been hampered because the GA product binds too weakly to reach saturation (26; data not shown). Nevertheless, a quantitative characterization of the reverse reaction is necessary to maximize our understanding of active site interactions and to relate the informa-

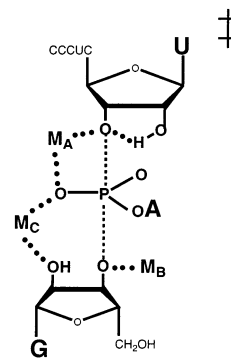


FIGURE 1: Metal ion interactions at the active site of the *Tetrahymena* group I ribozyme in the transition state. Figure according to Shan et al. (3).

tion about the ribozyme reaction to self-splicing. The reactants in the reverse reaction are analogues of the self-splicing intermediate, and the reverse reaction is analogous to the second chemical step in self-splicing (Scheme 1).

Previous work by Turner and co-workers and by this laboratory has suggested that binding of UCGA would be stronger than binding of GA due to formation of a short duplex with the ribozyme, referred to as P9.0 (25, 26, 34, 46). This duplex helps to position the 3'-exon in the second step of self-splicing. Furthermore, previous work also showed that the formation of these additional base pairs is compatible with catalysis (25, 34). UCGA was therefore used to investigate the reverse reaction (Figure 2A). Comparison of the substrate part of the framework with previously published data using guanosine (Figure 2B and below; refs 6, 37, and 43) shows that there are no qualitative differences. As with G, cooperative binding of substrates was observed in the presence of UCG (Figure 2B and below). Furthermore, using UCG instead of G accelerates the reaction of the ternary complex E•S•[UC]G only 2-fold (with rSA and -1d,rSA substrate; data not shown). These observations suggest that the reaction kinetics and thermodynamics are at most modestly affected with UCG instead of G (see also ref 34).

For historical reasons most previous mechanistic work on the forward reaction was carried out at 50 °C, with some of the more recent work performed at 30 °C (3, 6, 13, 37, 43, 47). However, the energetic effect from the P9.0 base pairs is only observed below 50 °C (data not shown). The experiments herein were therefore performed at 30 °C. To allow for comparison of the reverse and forward reaction, we also remeasured the kinetics and thermodynamics of the forward reaction at 30 °C (37), replacing G with UCG as the nucleophile. This allowed establishment of a framework of the L-21 *ScaI* ribozyme reaction in both directions under identical conditions. This framework is summarized in Figure 2B, and the experiments that yield these rate and equilibrium constants are described below. The forward reaction is described briefly, as we have followed previous experimental approaches (6, 37), except with UCG replacing G. We then describe in more detail dissection of the steps in the reverse reaction.

(A) *The Forward Reaction.* All experiments were performed under single-turnover conditions with the ribozyme in excess of the radiolabeled 5'-splice site analogue (*S) following methods described previously (6, 37). Association rate constants were determined from reactivity measurements

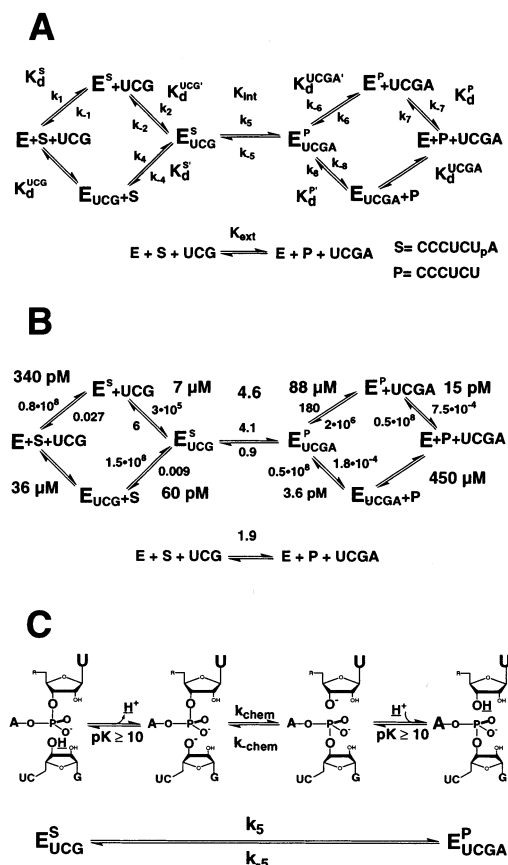


FIGURE 2: Kinetic and thermodynamic framework for the *Tetrahymena* L-21 *ScaI* ribozyme reaction. (A) Definition of rate and equilibrium constants used in the text. (B) Kinetic and thermodynamic framework at 30 °C, 10 mM MgCl₂, and pH 6.2, defined as described in Results and Materials and Methods. Association rate constants (k_1 , k_2 , k_4 , k_6 , k_7 , and k_8) are reported in M⁻¹ min⁻¹; all other rate constants are in units of min⁻¹. The reported dissociation rate constant of P from E·P·UCGA was calculated from the observed dissociation rate constant for Δ P and assuming that the effect of the 5'-most nucleotide is identical in E·P·UCGA and E·P (see Materials and Methods). The rate constants for the chemical step (k_5 and k_{-5}) were measured with the all-ribose oligonucleotides, rSA and rP, as were the association rate constants for S and P. For technical reasons the dissociation rate constants were measured with $-1d,rSA$ and $-1d,rP$. Previous results show that the identity of the 2'-OH has about a 3-fold effect on binding, attributed to duplex stability effects, and the effect is on the dissociation rate constant (38, 47). The rate constants for binding and release of UCG and UCGA (k_2 , k_{-2} , k_6 , and k_{-6}), included for completeness, will be described elsewhere (K. Karbstein and D. Herschlag, manuscript in preparation). (C) Expanded view of the conversion between bound substrates and products, as described by the rate constants k_5 and k_{-5} in part A.

as a function of ribozyme concentration, and dissociation rate constants were determined in pulse–chase experiments as described in Materials and Methods. The affinity of S for the free ribozyme (E) and for the E·UCG complex was calculated from the dissociation and the association rate constants. This was necessary because the affinity for S is so high (<1 nM) that nonspecific loss of ribozyme to tube walls occurs over the concentration range that would be needed to directly measure the dissociation constants. The affinity of UCG for E and E·S was determined from UCG concentration dependences of the reaction rate under conditions in which equilibration of bound UCG is rapid relative to subsequent reaction (see Materials and Methods).

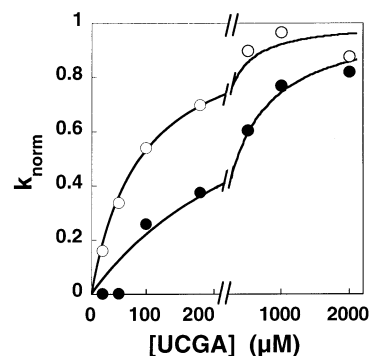


FIGURE 3: Cooperative binding of P and UCGA. Dependence of the reaction of E·P (○) or E + P (●) on UCGA concentration obtained at 10 mM MgCl₂, pH 7.7, as described in Materials and Methods. For comparison, the data were normalized. Nonlinear least-squares fitting to a single binding site model (eq 4) yielded binding constants of 89 ± 14 and 358 ± 110 μM for binding to E·P and E, respectively.

As observed previously with guanosine as the nucleophile, the substrates (S and UCG) bind cooperatively (11, 37, 43). That is, binding of each of the substrates is stronger when the other substrate is bound, relative to binding of that substrate alone ($K_d^S = 340$ pM and $K_d^{S'} = 60$ pM in the absence and presence of UCG, respectively, and $K_d^{UCG} = 36$ μM and $K_d^{UCG'} = 7$ μM in the absence and presence of S, respectively; Figure 2B).

(B) *The Reverse Reaction.* The affinity of the UCGA product for the free ribozyme and for the E·P complex was determined from concentration dependences of the reaction rate in single-turnover experiments (Figure 3). As observed previously for binding of UCG relative to G (26, 34), UCGA was bound at least 7-fold more strongly than GA (data not shown).

Binding of UCGA to the E·P complex was 5-fold stronger than binding to the free ribozyme ($K_d = 88$ vs 450 μM), suggesting that binding of one product strengthens binding of the other. This is analogous and similar in magnitude to the cooperativity observed between the substrates (11, 37, 48; see also The Forward Reaction above).

To independently test the model that the products bind cooperatively, we measured the dissociation constant for P in the presence and absence of bound UCGA. If P binding strengthens binding of UCGA, then UCGA binding must also strengthen binding of P. Because binding of P is very strong, it was not possible to determine its K_d by varying ribozyme concentration. (As noted above, these measurements are confounded by nonspecific loss of RNA to tube walls.) Instead, we obtained the affinity for P from the association and dissociation rate constants, as described below.

Association rate constants for P in the presence and absence of UCGA were determined from reactivity measurements as described in Materials and Methods. The presence of UCGA has essentially no effect on the association rate constant of P ($k_7 = k_8 = 0.5 \times 10^8$ M⁻¹ min⁻¹; Figure 2B). To determine the dissociation rate constant for P in the presence and absence of UCGA, pulse–chase experiments were performed as described in Materials and Methods. The experiments were complicated because in the presence of UCGA dissociation of $-1d,rP$ from the ternary complex E·P·UCGA is slower than reaction to form $-1d,rSA$. As a result, $-1d,rP$ does not persist long enough to follow its

dissociation, and the dissociation rate constant for in situ formed $-1d,rSA$ is measured instead. To circumvent this problem, it was necessary to increase the dissociation rate without affecting coupling and/or reactivity by using a modified form of P. Previous work had shown that shortening of the substrate by one residue at the 5'-end increases the dissociation rate constant, due to loss of one base pair, but does not affect other reaction steps (36, 37). This suggested that it would be possible to measure the effect of UCGA on the dissociation rate using a 5'-shortened form of the product, CCUCdT, which we term ΔP .

As expected for cooperative binding of products, dissociation of ΔP was slowed in the presence of UCGA ($k_{\text{off}}^{\Delta P} = 0.032$ and 0.008 min^{-1} in the absence and presence of UCGA, respectively). To allow comparison of homologous substrates and products, we also determined the dissociation rate constant of full-length product ($-1d,rP$) in the absence of UCGA ($k_{\text{off}}^P = 7.5 \times 10^{-4} \text{ min}^{-1}$) and calculated the dissociation rate constant for $-1d,rP$ in the presence of UCGA (Figure 2B), assuming that UCGA has the same 4-fold effect on the dissociation rate constant for P as it has on ΔP (see above).

Dissociation constants for P in the absence and presence of UCGA were obtained from the measured association and dissociation rate constants. The stronger binding of P in the presence of bound UCGA ($K_d = 15$ and 3.6 pM in the absence and presence of UCGA, respectively; Figure 2B) quantitatively confirms the cooperative binding of UCGA and P, which was suggested by the stronger binding of UCGA in the presence of P.

Previous studies suggested qualitatively that the two products of the reaction bind cooperatively (25). However, interpretation of these data is complicated by the possibility that a large fraction of the ribozyme was misfolded, as the ribozyme was not prefolded under conditions now known to be required for complete folding to the native conformation (35). Furthermore, these pioneering studies were undertaken with the 5'-exon analogue CUCU (25). Recent work shows that the rate-limiting step for this 5'-exon analogue is its docking into the active site and not the chemical step (36 and data not shown). Thus, the K_m values reported in these studies may not reflect K_d values.

Using the L-21G414 ribozyme, a version of the L-21 *ScaI* ribozyme that supplies guanosine in cis (G414), Mei and Herschlag (21) showed that dissociation of P from the ribozyme with G414 in the active site (resembling $E \cdot P \cdot UCG$) was 15-fold faster than dissociation of P from the ribozyme with G414A₅ in the active site (resembling $E \cdot P \cdot UCGA$). This was consistent with coupling between binding of G414A₅ and P in the active site. However, all or part of the observed effect could have arisen from anticoupling between G414 and P in the active site.

(C) *The External and Internal Equilibrium.* The external equilibrium constant, K_{ext} , describes the equilibrium between $E + S + UCG$ and $E + P + UCGA$ in solution (eq 6A). This equilibrium constant was determined from the extent of reaction with different ratios of UCGA/UCG under conditions in which substrates and products are subsaturating and therefore not significantly bound to ribozyme. Because binding of ribose-containing S and P is very strong (see previous section and Figure 2B), it was not possible to work at concentrations below the K_d without having problems of

Table 1: Internal and External Equilibrium Constants^a

| +1 residue | K_{int} | K_{ext} | ratio |
|-----------------|------------------|------------------|---------------|
| A | 4.6 ± 1.2 | 1.9 ± 0.2 | 2.4 ± 0.9 |
| CH ₃ | 5.2 ± 1.2 | 2.0 ± 0.2 | 2.6 ± 0.9 |

^a The +1 refers to the residue 3' to the cleavage site (Chart 1). K_{int} describes the equilibrium between bound substrates and products (eq 5A), and K_{ext} describes the equilibrium between substrates and products in solution (eq 6A). Errors in the equilibrium constants were estimated from the errors in the nonlinear least-squares fit. The error in the ratio was calculated by propagation of error.

nonspecific RNA losses and reactions slower than ribozyme degradation. We therefore used deoxyribose analogues of S and P ($-1r,dSA_5$ and $-1r,dP$), which bind weakly, such that useable concentrations of ribozyme ($\geq 2 \text{ nM}$) are subsaturating. Control experiments described in Materials and Methods strongly suggest that the equilibrium constants obtained with the deoxyribose-containing analogues provide accurate estimates of the equilibrium constants with the all-ribose oligonucleotides.

The value for the external equilibrium constant K_{ext} of 1.9 (Table 1) is close to unity, as expected for this symmetrical reaction with one phosphate diester replacing another; the only difference is the residue 5' to the transferred A-tail, which is either a U or a G (with S and P, respectively). Furthermore, the same value for the external equilibrium constant was observed for substrates in which the A-tail is replaced with a CH₃ group (Table 1). This suggests that differential stacking of the A-tail onto the U or G is not the reason for the small perturbation from unity.

The internal equilibrium constant, which describes the equilibrium between $E \cdot S \cdot UCG$ and $E \cdot P \cdot UCGA$ (eq 5A), was measured as the quotient of the reaction rates in the forward and reverse reaction (eq 5B). A value of $K_{\text{int}} = 4.6$ was obtained. As described in Materials and Methods, the forward and reverse reaction rate constants were determined under conditions in which both substrates (or both products) are saturating and under which the chemical step is rate-limiting. Furthermore, the reaction rate constants were measured at several different low pH values and were found to be log-linear with a slope of 1 (data not shown), suggesting that the chemical step was indeed rate-limiting (41, 42). In addition, the internal equilibrium constant was measured independently from the fraction of reacted substrate in reactions with UCG and UCGA added together at saturating concentrations. The methods agreed within 20%.

The value for the internal equilibrium constant of 4.6 is only ~ 2 -fold different from the value of the external equilibrium constant (Table 1). This small difference is the result of a larger destabilization of S relative to P (20-fold) compared to the destabilization of UCGA relative to UCG (12-fold).

The same value for the internal equilibrium constant is obtained when the A-tail is replaced with a CH₃ tail (Table 1), suggesting that differential stacking of the A-tail in the ternary complexes does not contribute to the slight stabilization of $E \cdot P \cdot UCGA$ on the ribozyme. These results demonstrate that, under these conditions, this ribozyme does not provide substantial preferential stabilization of the substrates or products.

The internal equilibrium constant can also be independently calculated from the external equilibrium constant and

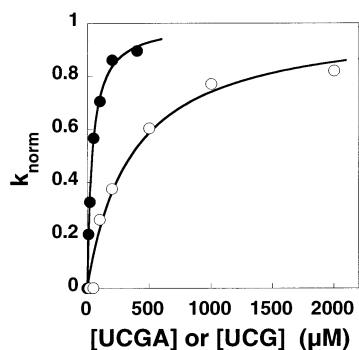


FIGURE 4: UCGA binds weaker to free ribozyme than UCG. UCG concentration dependence of the rate of reaction from E + S (●) and UCGA concentration dependence of the rate of reaction from E + P (○), determined as described in *Materials and Methods* at 10 mM MgCl₂, 30 °C. For comparison, the data were normalized. Nonlinear least-squares fitting to a single binding site model (eq 4) yielded binding constants of 35 ± 2 and 358 ± 110 μM for UCG and UCGA, respectively.

the binding constants for substrates and products according Figure 2A. This was possible because equilibrium constants that are thermodynamically related to one another were each experimentally measured. Four independent calculations of the internal equilibrium constant (all combinations of the bottom and top pathways in Figure 2B) give an average value of $K_{\text{int}} = 3.0 \pm 0.5$, close to the directly measured value of 4.6. This provides a quantitative demonstration of the internal consistency of the framework in Figure 2B.

Origin of the Difference in Binding of UCGA Relative to UCG. The observation that UCGA bound more weakly than UCG (Figure 4; see also ref 21) suggested a difference in the binding interactions of these ligands. To understand these interactions, it was necessary to probe the molecular origin for the weaker binding of UCGA. To do this, we wanted to know which part of UCGA was responsible for the weaker binding of UCGA relative to UCG.

(A) *Testing an Unfavorable Interaction with the A 3' to the Cleavage Site.* To test whether the reason for the destabilization of UCGA relative to UCG was an unfavorable interaction with the A 3' to the cleavage site, a UCGA analogue in which the A was replaced with a methyl group (CUCG_pMe) was used. Binding constants could not be measured directly as insufficient quantities of CUCG_pMe were available. Therefore, an alternative approach was necessary to compare the binding affinities for UCGA and UCG_pMe.

Substitution of the A 3' to the cleavage site with a methyl group has no effect on the external equilibrium (Table 1). Thus, free substrates and products have the same free energy difference regardless of whether the 3'-group is an A or a CH₃. Also, binding of G or P to free ribozyme is by definition not affected by the presence of a 3'-A or CH₃ group on S or UCG, so that E•G and E•P are also unaffected relative to the free species. Finally, the internal equilibrium is unaffected by substituting the 3'-A with a CH₃ group (Table 1). This provides a thermodynamic relationship that constrains the ratios of binding of UCGA versus CCCUCUA and UCG_pMe versus CCCUCU_pMe to be the same. Previous work showed that CCCUCU_pMe was bound ~4-fold more weakly than CCCUCUA (12). Thus, binding of UCG_pMe is ~4-fold weaker than binding of UCGA.

Table 2: Binding of Guanosine Analogues to Free Ribozyme^a

| G analogue | 10 mM MgCl ₂ | | 2 mM MgCl ₂ | |
|------------|-------------------------|------------------|------------------------|------------------|
| | K_d (μM) | K_{rel} | K_d (μM) | K_{rel} |
| G | 400 | (1) | 970 | (1) |
| 3'dG | ≥ 13000 | ≥ 33 | ≥ 10000 | ≥ 10 |
| UCG | 36 | (1) | 66 | (1) |
| UCGA | 450 | 13 | 250 | 4 |

^a K_d values were determined from concentration dependences of reaction rates at 30 °C. Due to limited solubility only a lower limit could be determined for 3'dG.

A more direct comparison of CUCGA and CUCG_pMe affinities can be made as Mn²⁺ strengthens binding of these oligonucleotides sufficiently to allow binding constants to be measured. In the presence of 10 mM Mn²⁺ and 10 mM Mg²⁺, CUCGA binds about 2-fold tighter than CUCG_pMe (A. Kravchuk and D. Herschlag, unpublished results). A previous report in the literature suggested that UCGA and UCGU bind with the same affinity (26), consistent with the findings reported here.

In summary, these data strongly suggest that unfavorable interactions with the A-tail are not responsible for the weaker binding of UCGA.

(B) *Testing Destabilization Arising from a Metal Ion.* Another possible model for the weaker binding of UCGA relative to UCG was that the metal ion that binds next to the 3'-oxygen of UCG, metal ion B (Figure 1),² destabilizes binding of UCGA relative to UCG. There could be an electrostatic effect between metal ion B and the 3'-oxygen attached to G in UCGA. This is because the electron-withdrawing phosphoryl group in UCGA is expected to decrease the negative charge potential at the 3'-oxygen relative to a hydrogen atom (in UCG). An analogous model was suggested previously to account for the stronger binding of P relative to S (12).

If metal ion B were solely responsible for the destabilization of UCGA relative to UCG, it would be expected that, in the absence of metal ion B, UCG and UCGA would bind with similar affinity. Previous work provided an estimate of the K_d for metal ion B of ~6 mM (1). Thus, this metal ion will not be stably bound at 2 mM Mg²⁺. We therefore compared the affinities for UCG and UCGA in 2 mM MgCl₂.

In the absence of metal ion B, binding of UCGA is less destabilized (relative to UCG) than in the presence of metal ion B ($K_{\text{rel}}^{\text{UCGA}} = 13$ and 4 at 10 and 2 mM Mg²⁺, respectively; Table 2). The less pronounced destabilization is partly due to weaker binding of UCG at 2 mM Mg²⁺ and partly due to somewhat stronger binding of UCGA at 2 mM Mg²⁺ (Table 2). The simplest model from these results is that a modestly destabilizing interaction is made with metal ion B. It is also possible that the observed effect is indirect and the result of a conformational change in the ribozyme that occurs between 2 and 10 mM MgCl₂. Nevertheless, the destabilization arising from metal ion B is small in magnitude, and UCGA binding remains weaker relative to UCG at 2 mM Mg²⁺.

² The nomenclature for active site metal ions established by Shan and Herschlag (1, 2) is used throughout to refer to individual metal ions. In this nomenclature metal ion A binds to the 3'-oxygen of U(-1), metal ion B binds to the 3'-oxygen of G, and metal ion C binds to the 2'-hydroxyl of G (see Figure 1).

(C) *Testing Stabilization of UCG Binding through the 3'-OH.* To account for the residual destabilization of UCGA relative to UCG at low Mg^{2+} , we considered a model in which UCG was bound stronger than UCGA because it forms a hydrogen bond between the 3'-OH and a residue on the ribozyme. We tested this possibility by comparing the affinity of G with the affinity of 3'dG, a compound in which the 3'-OH group was replaced with a hydrogen atom. Like [UC]-GA, 3'dG cannot donate a hydrogen bond. G and 3'dG were used in these experiments because UC(3'dG) was not available. To account for the stronger binding due to formation of P9.0, we compared 3'dG binding to G binding and UCG binding to UCGA binding (K_{rel}). The affinity for 3'dG and G was measured in the presence of 2 mM $MgCl_2$, such that metal ion B, which binds to the 3'-group on G, was not present (1). This was important because, otherwise, binding of 3'dG might be weak because of the unfavorable interaction of the hydrophobic 3'-H and the charge on the metal ion (Table 2).

Since 3'dG is not reactive (44, 45; data not shown), its affinity was measured by inhibition using a subsaturating concentration of G as described in Materials and Methods. Inhibition of only ~35% was observed up to the highest attainable concentration of 3'dG, so that only a lower limit for the dissociation constant could be obtained.

As summarized in Table 2, changing the 3'-OH to a 3'-H or a 3'-OA weakens binding ($K_{rel}^{3'H} = 10$ and $K_{rel}^{3'OA} = 4$ in the presence of 2 mM Mg^{2+}). The simplest interpretation of these data is that the 3'-OH is engaged in a hydrogen bond to a residue on the ribozyme that increases the affinity of UCG relative to UCGA and of G relative to 3'dG.

Probing the pK_a Value of the 3'-Hydroxyl Group of G and U(-1) of P. Phosphoryl-transfer reactions such as the ribozyme reaction require loss of a proton from the attacking group and gain of a proton by the leaving group. This is illustrated in Figure 2C, which expands the central part (k_5 and k_{-5}) of the reaction scheme from Figure 2A. For the *Tetrahymena* L-21 *ScaI* ribozyme, metal ions bound to the nucleophile and the leaving group have been suggested to facilitate deprotonation of the nucleophile and provide electrostatic stabilization of the leaving group (1, 3, 49, 50). This has been proposed to be a major catalytic strategy for other ribozymes as well (e.g., refs 51–54). We probed the pK_a of the nucleophile for the forward and the reverse reaction [3'-OH on G and U(-1), respectively] to understand how large the contribution from nucleophilic activation by metal ions is compared to the overall rate enhancement by the L-21 *ScaI* ribozyme.

Using the information from the highly defined framework, it is possible to find conditions under which the deprotonation of the nucleophile (3'-OH on G) or the leaving group [3'-OH at position U(-1) on P] can be probed (Figure 2C) by following the pH dependence of the reaction rate of the forward reaction under conditions in which the chemical step is rate-limiting.

The reaction rate constant for reaction from the $E \cdot S \cdot UCG$ ternary complex was measured as a function of pH as described in Materials and Methods. The dependence of the reaction rate constant on pH shows no significant curvature up to pH 9.4 (Figure 5), placing a lower limit for the pK_a of the 3'-OH of G of ≥ 10 . This limit is consistent with the

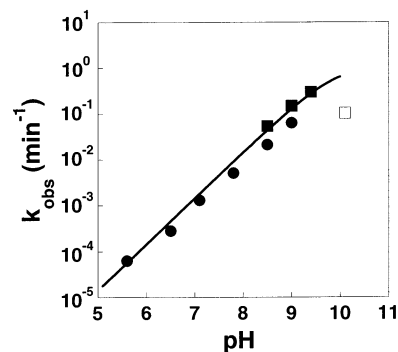


FIGURE 5: The pK_a value of the nucleophilic 3'-OH of G is ≥ 10 . The pH dependence for the reaction from $E \cdot S \cdot G \rightarrow$ products was obtained at 4 °C, 2 mM G, and 100 mM $MgCl_2$ using the $-1d,rSA_5$ substrate. The circles and squares represent data from independent experiments. The line shows a nonlinear least-squares fit of all data, except the open symbol, by eq 8 (see Materials and Methods) and yielded a lower limit for an apparent pK_a of 10. The data point represented by the open symbol was excluded because the decreased extent of reaction suggests that the lower cleavage rate is caused by unfolding of the ribozyme (41) and/or inactivation due to hydrolysis at this high pH value (data not shown).

previously obtained lower limit of ≥ 8.2 (41). At higher pH values there was a drop in activity, presumably due to disruption of the structure (41) and/or ribozyme degradation (Figure 5 and data not shown).

Experiments in which the pK_a of the 3'-OH on U(-1) was probed by reaction of $E \cdot P \cdot GUCGA$ show that the internal equilibrium, which is a function of the ratios of the rate constant for the forward and the reverse reaction, is unchanged up to pH 9.4 (Figure S1, Supporting Information). This suggests that the pH dependence for the reverse step is analogous to the pH dependence for the forward reaction. Thus, the same lower limit of $pK_a = 10$ was obtained for the pK_a of the 3'-OH on U(-1).

DISCUSSION

The L-21 *ScaI* ribozyme is derived from the self-splicing *Tetrahymena* group I intron and serves as a model for the self-splicing reaction. Previous characterization of the reaction mostly involved the forward reaction, a model for the first step of self-splicing, and yielded detailed mechanistic insights into the reaction (e.g., refs 1, 3, 6, 9–13, 19, 20, 40, 48, 55, and 56). However, the reverse reaction is equally important, as the ribozyme reaction products are analogues of the self-splicing intermediates and the reverse reaction is a model for the second step of self-splicing (Scheme 1). Characterizing the kinetics and thermodynamics of the reverse reaction therefore provides an important link between the ribozyme and the self-splicing reactions and will be essential for applying the extensive knowledge of the ribozyme reaction toward understanding how the RNA facilitates the more complex multistep self-splicing reaction.

Framework for the L-21 ScaI Reaction in Both Directions. In the work presented herein, we have established a framework for the forward and reverse reactions of the L-21 *ScaI* ribozyme under uniform conditions (Figure 2B). The validity and accuracy of this framework are supported by the agreement between equilibrium constants determined directly and calculated from other equilibrium constants with use of thermodynamic relationships within the framework.

Comparisons of binding affinities of substrates and products have revealed a new interaction at the active site (see Origin for UCGA Destabilization below). Furthermore, we have used the information from the framework to probe the pK_a value of the nucleophiles in the forward and reverse reaction (see Metal Ions for Activation of Nucleophiles in RNA Catalysis below).

Examining the framework for the L-21 *ScaI* reaction in both directions has revealed analogies between the forward and reverse reactions: cooperative binding, destabilization from the reactive phosphoryl group, and similar rate enhancements in both directions.

Substrates as well as products bind cooperatively to the ribozyme with similar binding enhancements of ~ 5 -fold ($K_d^S/K_d^{S'} \approx K_d^{UCG}/K_d^{UCG'} \approx K_d^P/K_d^{P'} \approx K_d^{UCGA}/K_d^{UCGA'} \approx 5$; Figure 2B). Cooperative binding of substrates was shown to involve a conformational change in the ribozyme (11, 37, 48). Further investigations will be required to determine whether cooperative product binding also involves a conformational change or instead a direct interaction between the products.

The 5'-splice site analogue S, which contains the reactive phosphoryl group, binds 20-fold less strongly than the 5'-exon analogue P (12 and Figure 2B). Binding of UCGA and UCG behaves analogously, with UCGA binding 12-fold less strongly than UCG (Figure 2B; see also ref 21). The difference in the destabilization of S relative to P and UCGA relative to UCG accounts for the observed 2-fold perturbation in the internal equilibrium constant relative to the external equilibrium constant ($K_{int} = 4.6$ versus $K_{ext} = 1.9$).

The similar rate constants for reaction of bound substrates and bound products and the overall reaction symmetry, in which one 3'-5'-phosphodiester bond is replaced by another, indicate that the rate enhancement for the forward and reverse reactions is essentially the same.

Implications for Self-Splicing. After the first step of self-splicing, the exogenous G nucleophile has added onto the 5'-end of the intron-3'-exon intermediate, and the cleaved 5'-exon presumably stays bound to ensure exon ligation rather than loss of free 5'-exon (6, 21, 57). Consistent with previous suggestions (21, 25, 26), the results herein show that the esterified guanosine, in a complex that mimics this intermediate, has a lower affinity for the active site than free guanosine in the first step. The affinity decrease may provide a driving force for removal of the esterified guanosine from the active site after the first step in self-splicing and its replacement by the guanosine that specifies the 3'-splice junction. As the 3'-splice site guanosine is also esterified, additional pairing interactions in P9.0 and P10 may be required to stabilize its binding in the active site (26, 34, 46; unpublished results).

The equilibrium constant for the overall ribozyme reaction, referred to as K_{ext} herein, is close to unity, as is the "internal equilibrium" for conversion of bound substrates and products (K_{int}). The latter observation was made previously (21) using a different form of the L-21 ribozyme (L-21G414) that supplies guanosine in cis (G414). It will be of interest to ascertain whether these equilibria are perturbed by conformational changes throughout the self-splicing reaction.

Origin of Differential Binding of UCG and UCGA. From the previous observation of weaker binding of S than P it was suggested that the electron-withdrawing phosphoryl group weakened an electrostatic interaction between a metal

ion and the bridging 3'-oxygen (Figure 1, M_A). This interaction would provide ground-state destabilization relative to interactions with solvent that would be removed as the oxygen accumulated negative charge in the transition state, thereby contributing to catalysis (12). Because metal ion A is bound under conditions needed to form the active ribozyme structure [~ 2 mM Mg^{2+} (1)], it was not possible to determine the effect of removing this metal ion; i.e., if the metal ion were responsible for the observed destabilization, then, in the simplest case, removal of the metal ion would abolish the destabilization. In contrast, metal ion B, situated adjacent to the nucleophilic 3'-oxygen of UCG, binds weakly, with an apparent dissociation constant of 6 mM (1). Thus, metal site B is expected to be largely unoccupied at 2 mM Mg^{2+} . This allowed us to test the role of metal ion B in the weaker binding of UCGA than UCG.³

Binding experiments indicated that weaker binding of UCGA than UCG was maintained at 2 mM Mg^{2+} , although part of the destabilization was relieved (Table 2). Removal of the 3'-OH group of guanosine and replacement with a hydrogen atom substantially destabilizes binding (Table 2). Destabilization cannot be traced to the 3'-A of UCGA, as replacement of this A residue with a methyl group gave no relief of the destabilization.

The simplest interpretation of these data is that an electrostatic interaction with metal ion B contributes to the weaker binding of UCGA relative to UCG ($K_{rel}^{3'OA} = 4$ and 13 at 2 and 10 mM Mg^{2+} , respectively) but this interaction cannot fully account for the destabilization. The stronger binding of guanosine than 3'dG suggests the presence of a ground-state interaction with the 3'-hydroxyl group. This hydroxyl group could donate a hydrogen bond to a group on the ribozyme, an interaction that would be prevented upon phosphorylation, or it could accept a hydrogen bond, an interaction that would be weakened or could be sterically precluded by the electron-withdrawing phosphoryl group. Accepting a hydrogen bond could contribute to catalysis by stabilizing charge development of the 3'-oxygen atom in the transition state, whereas hydrogen bond donation implies a nonproductive binding interaction that would need to be broken to achieve the reaction's transition state (Figure 2C).

The weaker binding of 3'dG relative to UCGA ($K_{rel}^{3'H} \geq 10$ and $K_{rel}^{3'OA} = 4$ relative to G and UCG, respectively) might be the result of the lack of the phosphoryl oxygens in 3'dG. The *pro-R_p* phosphoryl oxygen appears to be involved in transition state interactions with two metal ions stably bound to the ribozyme, so its presence could increase the affinity of UCGA relative to 3'dG (3, 56). Alternatively, ~ 3 -fold weaker binding of 3'dG relative to UCGA could be accounted for by the opposite sugar preferences of these

³ Figure 1 depicts a model for active site interactions derived from extensive quantitative probing of metal ion interactions via single atom substitutions within the substrates and variation in the metal ion concentrations and identities (1, 3). Nevertheless, it remains possible that there is a more complex explanation for the observed behavior and a different model holds in which another unidentified metal ion interacts with the 3'-OH in addition to (or instead of) metal ion B. Such a metal ion could be present even at 2 mM Mg^{2+} and be responsible for the weaker affinity of 3'dG and UCGA that remains at low Mg^{2+} . Whereas this model cannot be ruled out, we have no indication of interactions of more than one metal ion with the 3'-oxygen at G, and all data are consistent with metal ion B directly contacting the 3'-oxygen at G (1, 3).

species, if binding occurred in the 2'-endo conformation (26, 58). It should be noted that the same guanosine ring conformation is favored for UCG and UCGA, so that sugar pucker is unlikely to account for the stronger UCG binding (Table 2).

In summary, these data are consistent with an interaction of the 3'-moiety of UCGA with metal ion B that makes a small contribution to the destabilization of UCGA relative to UCG and also suggest the presence of a hydrogen bond between the 3'-OH of UCG and the ribozyme active site.

Metal Ion Activation of Nucleophiles in RNA Catalysis. Metal ions are commonly found in protein enzymes that catalyze phosphoryl-transfer reactions, such as restriction endonucleases and DNA and RNA polymerases (e.g., refs 59–62). One of the mechanisms by which these metal ions could facilitate a reaction is by lowering the pK_a of the attacking nucleophile to increase the concentration of the more reactive oxyanion species. In addition, metal ions can stabilize the negative charge that develops on the leaving group in the transition state for phosphoryl transfer (63–66). Because RNA is adept at binding metal ions and because many RNA-catalyzed reactions are phosphoryl-transfer reactions, it has been speculated that ribozymes accelerate these reactions by providing a scaffold to bind metal ions, which contribute to the rate enhancement by mechanisms such as activating the nucleophile and stabilizing the leaving group (20, 67; see also refs 51 and 52).

The interconversion of L-21 *ScaI* ribozyme-bound substrates and products is depicted in Figure 2C. This model of the reaction is based on the observation of a log-linear pH dependence with a slope of 1, which suggests a single deprotonation prior to the transition state, and the evidence for functionally important metal ions bound to the nucleophiles in the forward and reverse reaction (1, 3, 49, 50). The simplest interpretation of these data is that the metal ions rather than a general acid or general base activate the nucleophile or stabilize the leaving group and that the observed pH dependence is due to deprotonation of the 3'-OH of the nucleophile in each direction.

Due to the high pK_a of the 3'-OH ($pK_{a,solution} \approx 13$),⁴ only 1 in $\sim 10^6$ guanosine molecules is in the active deprotonated form at neutral pH. Lowering the pK_a of the 3'-OH on guanosine to match the physiological pH of ~ 7 could provide a rate enhancement of ~ 4 orders of magnitude. This is because a much higher fraction of guanosine molecules would be in the deprotonated form at neutral pH [some of this increase in concentration is offset because the lower pK_a nucleophile is less reactive (8, 68)]. To understand the importance of activating the nucleophile for the group I ribozyme reaction, the pK_a value of the nucleophilic 3'-OH on G (and the 3'-OH on U(-1) for the reverse reaction) bound to the ribozyme needs to be compared to the solution pK_a value of ~ 13 .

⁴ The estimate for the solution pK_a of ~ 13 for the 3'-OH on RNA derives from the following comparisons: The pK_a difference between alcohols and thiols is ~ 5 units [methanol vs methanethiol, $\Delta pK_a = 4.9$; ethanediol vs mercaptoethanol, $\Delta pK_a = 5.0$ (4)]. Adding this ΔpK_a of ~ 5 to the observed solution pK_a value for 3'-thio P of 8.4 (A. Yoshida and J. Piccirilli, personal communication) yields an estimate for a solution pK_a value of ~ 13 for the 3'-OH. This value is similar to the observed pK_a value for 2'-OH of ~ 12.5 (5).

Previous work provided a lower limit of 8.2 for the pK_a of the ribozyme-bound 3'-OH on G (41). Here we have extended previous measurements and determined a lower limit of 10 for the pK_a of the 3'-OH of G and of P, the nucleophiles in the forward and reverse ribozyme reaction, respectively (see Figure 2C). Comparing the pK_a of the 3'-OH moieties in solution and bound on the enzyme ($pK_{a,solution} \approx 13$ and $pK_{a,enzyme} \geq 10$) shows that the ribozyme-bound Mg^{2+} ions perturb the pK_a of the 3'-OH by at most ~ 3 units; Mg^{2+} perturbs the pK_a of water by ~ 3.5 units.⁵ This comparison suggests that binding to the ribozyme does not influence the electrostatic behavior of the bound Mg^{2+} ions to provide greater stabilization of the oxyanion than Mg^{2+} ions in solution. Nevertheless, the observation of a 2 unit perturbation of the pK_a of a 3'-SH on U(-1) in the presence of Mn^{2+} bound at site A (A. Yoshida and J. A. Piccirilli, personal communication) indicates that metal ions can indeed facilitate the deprotonation of the 3'-group on U(-1).

The results described above suggest that ribozyme-bound Mg^{2+} ions are not intrinsically better at stabilizing negative charge than Mg^{2+} ions that interact with a negatively charged group in solution. However, weak ligands such as the 3'-hydroxyl groups of nucleic acids cannot compete effectively with water for interaction with metal ions. The ribozyme provides an advantage as it can bind and position the metal ion and the nucleophile with respect to one another (12), thereby increasing the probability of deprotonation relative to the situation in solution.

Origin of the Catalytic Power of the L-21 ScaI Ribozyme. The rate enhancement for reaction of substrates bound to the *Tetrahymena* ribozyme is about 10^{11} -fold compared to a hydrolysis reaction and 10^{13} -fold⁶ compared to attack by guanosine in solution at a standard state of 1 M. To evaluate the catalytic power of the ribozyme, the ribozyme-catalyzed reaction was compared to the identical uncatalyzed reaction, i.e., attack of guanosine, and not the hydrolysis reaction, which is favored in solution. Below we examine the contribution of metal ion catalysis to the 10^{13} -fold rate enhancement for the L-21 *ScaI* reaction.

As described above, binding to the ribozyme-bound metal ion B could lower the pK_a of the nucleophile by up to 3 units. This could account for up to 10^2 -fold rate enhancement when the loss of nucleophile strength is taken into account (8, 68).

Further rate enhancement comes from metal ion stabilization of the developing negative charge on the leaving group in the transition state. The amount of stabilization of the negative charge in the transition state is approximated by the amount of stabilization of negative charge arising from deprotonation, described by the pK_a . Because the leaving group in the forward direction [3'-oxyanion on U(-1)] is the nucleophile in the reverse direction (Figure 2C), the upper

⁵ Mg^{2+} perturbs the observed pK_a of water by 4.3 units from 15.7 to 11.4. After a statistical correction to compare the probability of deprotonation of one of six bound waters to the probability of deprotonation of a single bound alcohol, this gives $\Delta pK_a = 3.5$.

⁶ Rate enhancements were estimated as described previously (6) using a second-order rate constant for attack of hydroxide on dimethyl phosphate monoanion of $8 \times 10^{-9} M^{-1} min^{-1}$ (7) and accounting for the pK_a differences in the leaving group (methanol versus the 3'-OH of ribose) with a $\beta_{lg} = -1$ (8) and for the differences in the nucleophile (hydroxide versus 3'-O⁻ of ribose) with a $\beta_{nuc} = 0.3$ (8).

limit for the pK_a perturbation of this group of 3 units provides an upper limit for the stabilization of the developing negative charge in the transition state. Together with the observed leaving group dependence of the reaction rate for phosphoryl-transfer reactions [$\beta_{lg} = -1$ (8)], this provides an upper limit of $\sim 10^3$ -fold rate enhancement from stabilization of the leaving group by bound metal ion A.⁷

An independent way to crudely assess the catalytic contributions from nucleophilic activation by metal ions is to determine the effect of replacing interacting oxygen atoms with sulfur. Sulfur substitution leads to a weakening or loss of interaction with Mg^{2+} ions. The thio effects from replacing the 3'-oxygen of G is 200-fold, and the thio effect from replacing the 3'-oxygen of U(-1) is 2000-fold in the forward and reverse reaction, respectively (1). The latter number overestimates the effect from loss of metal ion A, as this thio substrate, when bound, does not dock stably into the active site (2). On the other hand, there could be residual catalytic interactions between Mg^{2+} and sulfur. More generally, thio effects do not distinguish between loss of electrostatic activation of the nucleophile (or loss of electrostatic stabilization of the leaving group), loss of positioning, and loss of other catalytic interactions such as the stabilization of negative charge on the nonbridging phosphoryl oxygen atoms.

The estimates described above suggest that activation of the nucleophile and stabilization of the leaving group by binding of metal ions together could account for no more than $\sim 10^5$ -fold of the 10^{13} -fold rate enhancement by the *Tetrahymena* group I intron. Metal ions A and C could stabilize negative charge on one of the nonbridging phosphoryl oxygen atoms if such charge development occurs in the transition state. Such an effect from ionic interactions is likely to be substantially less than the ~ 300 -fold effect arising from alkylation of the phosphate diester to give a triester [from comparison of esters with leaving group pK_a 's of 10 (69)].

The analysis above suggests that through activation of nucleophile and leaving group, and possibly by stabilizing negative charge development on the nonbridging phosphate oxygens, metal ions provide substantial contributions to ribozyme catalysis. Nevertheless, metal ion catalysis cannot account for all of the catalytic power of this ribozyme. This is in keeping with recent work that has shown that several other ribozymes can catalyze reactions efficiently in the absence of divalent metal ions (e.g., refs 70–74). Additional catalytic strategies must therefore be employed by this and other ribozymes to achieve their large rate enhancements. For the *Tetrahymena* ribozyme, these mechanisms include stabilization of the negative charge on the leaving group oxygen in the transition state through a hydrogen bond between the 2'-OH and the 3'-oxygen on U(-1) (75) and repositioning of substrates within the active site of this ribozyme (e.g., refs 12 and 13).

The quantitative analysis of the contribution of metal ion activation of the nucleophile and leaving group together with

the previous body of work therefore suggests that, analogous to protein enzymes (e.g., refs 76–84), RNA enzymes use multiple catalytic strategies to achieve their enormous rate enhancements.

ACKNOWLEDGMENT

We thank James Hougland and Joe Piccirilli (University of Chicago) for the gift of CUCG_pMe, Aiichiro Yoshida and Joe Piccirilli for permission to cite unpublished data, and members of the Herschlag laboratory for helpful comments on the manuscript.

SUPPORTING INFORMATION AVAILABLE

Time courses for reactions of E•P•GUCGA at different pH values. This material is available free of charge via the Internet at <http://pubs.acs.org>.

REFERENCES

- Shan, S., Yoshida, A., Sun, S. G., Piccirilli, J. A., and Herschlag, D. (1999) *Proc. Natl. Acad. Sci. U.S.A.* 96, 12299–12304.
- Shan, S., and Herschlag, D. (2000) *RNA* 6, 795–813.
- Shan, S., Kravchuk, A. V., Piccirilli, J. A., and Herschlag, D. (2001) *Biochemistry* 40, 5161–5171.
- Jencks, W. P., and Regenstein, J. (1979) in *Ionisation Constants of Organic Acids in Aqueous Solution*, pp J187–J244, Pergamon Press, Oxford.
- Velikyan, I., Acharya, S., Trifonova, A., Foldesi, A., and Chatopadhyaya, J. (2001) *J. Am. Chem. Soc.* 123, 2893–2894.
- Herschlag, D., and Cech, T. R. (1990) *Biochemistry* 29, 10159–10171.
- Haake, P., and Westheimer, F. H. (1961) *J. Am. Chem. Soc.* 83, 1102–1109.
- Kirby, A. J., and Younas, M. (1970) *J. Chem. Soc. B*, 1165–1172.
- Cech, T. R., Herschlag, D., Piccirilli, J. A., and Pyle, A. M. (1992) *J. Biol. Chem.* 267, 17479–17482.
- Bevilacqua, P. C., Kierzek, R., Johnson, K. A., and Turner, D. H. (1992) *Science* 258, 1355–1357.
- McConnell, T. S., Cech, T. R., and Herschlag, D. (1993) *Proc. Natl. Acad. Sci. U.S.A.* 90, 8362–8366.
- Narlikar, G. J., Gopalakrishnan, V., McConnell, T. S., Usman, N., and Herschlag, D. (1995) *Proc. Natl. Acad. Sci. U.S.A.* 92, 3668–3672.
- Narlikar, G. J., and Herschlag, D. (1998) *Biochemistry* 37, 9902–9911.
- Strobel, S. A., OrtolevaDonnelly, L., Ryder, S. P., Cate, J. H., and Moncoeur, E. (1998) *Nat. Struct. Biol.* 5, 60–66.
- Slavi, B., Sullivan, M., Chance, M. R., Brenowitz, M., and Woodson, S. A. (1998) *Science* 279, 1940–1943.
- Treiber, D. K., Rook, M. S., Zarrinkar, P. P., and Williamson, J. R. (1998) *Science* 279, 1943–1946.
- Pyle, A. M., and Cech, T. R. (1991) *Nature* 350, 628–631.
- Strobel, S. A., and OrtolevaDonnelly, L. (1999) *Chem. Biol.* 6, 153–165.
- Szewczak, A. A., OrtolevaDonnelly, L., Ryder, S. P., Moncoeur, E., and Strobel, S. A. (1998) *Nat. Struct. Biol.* 5, 1037–1042.
- Narlikar, G. J., and Herschlag, D. (1997) *Annu. Rev. Biochem.* 66, 19–59.
- Mei, R., and Herschlag, D. (1996) *Biochemistry* 35, 5796–5809.
- Zaug, A. J., and Cech, T. R. (1986) *Science* 231, 470–475.
- Woodson, S. A., and Cech, T. R. (1989) *Cell* 57, 335–345.
- Bevilacqua, P. C., Johnson, K. A., and Turner, D. H. (1993) *Proc. Natl. Acad. Sci. U.S.A.* 90, 8357–8361.
- Bevilacqua, P. C., Sugimoto, N., and Turner, D. H. (1996) *Biochemistry* 35, 648–658.
- Moran, S., Kierzek, R., and Turner, D. H. (1993) *Biochemistry* 32, 5247–5256.
- Albery, W. J., and Knowles, J. R. (1976) *Biochemistry* 15, 5627–5631.
- Burbaum, J. J., and Knowles, J. R. (1989) *Biochemistry* 28, 9306–9317.

⁷ It remains possible that in the transition state the leaving group is stabilized to a greater extent than predicted from an observed pK_a value of ≥ 10 . This would occur if an alternative, nonproductive but more stable ground-state complex for E•P•UCGA existed, in which the presence of a 3'-OH on P were favored relative to a 3'-oxyanion.

29. Kuchta, R. D., Mizrahi, V., Benkovic, P. A., Johnson, K. A., and Benkovic, S. J. (1987) *Biochemistry* 26, 8410–8417.
30. Dahlberg, M. E., and Benkovic, S. J. (1991) *Biochemistry* 30, 4835–4843.
31. Boyer, P. D. (1987) *Biochemistry* 26, 8503–8507.
32. Wells, T. N. C., and Fersht, A. R. (1986) *Biochemistry* 25, 1881–1886.
33. Zaug, A. J., Grosshans, C. A., and Cech, T. R. (1988) *Biochemistry* 27, 8924–8931.
34. Russell, R., and Herschlag, D. (1999) *RNA* 5, 158–166.
35. Russell, R., and Herschlag, D. (1999) *J. Mol. Biol.* 291, 1155–1167.
36. Narlikar, G. J., Bartley, L. E., Khosla, M., and Herschlag, D. (1999) *Biochemistry* 38, 14192–14204.
37. Shan, S., and Herschlag, D. (1999) *Biochemistry* 38, 10958–10975.
38. Herschlag, D., Eckstein, F., and Cech, T. R. (1993) *Biochemistry* 32, 8312–8321.
39. Narlikar, G. J., and Herschlag, D. (1996) *Nat. Struct. Biol.* 3, 701–710.
40. Strobel, S. A., and Cech, T. R. (1993) *Biochemistry* 32, 13593–13604.
41. Knitt, D. S., and Herschlag, D. (1996) *Biochemistry* 35, 1560–1570.
42. Herschlag, D., and Khosla, M. (1994) *Biochemistry* 33, 5291–5297.
43. Knitt, D. S., Narlikar, G. J., and Herschlag, D. (1994) *Biochemistry* 33, 13864–13879.
44. Bass, B. L., and Cech, T. R. (1984) *Nature* 308, 820–826.
45. Bass, B. L., and Cech, T. R. (1986) *Biochemistry* 25, 4473–4477.
46. Michel, F., Hanna, M., Green, R., Bartel, D. P., and Szostak, J. W. (1989) *Nature* 342, 391–395.
47. Narlikar, G. J., Khosla, M., Usman, N., and Herschlag, D. (1997) *Biochemistry* 36, 2465–2477.
48. Shan, S., and Herschlag, D. (2002) *RNA* (in press).
49. Piccirilli, J. A., Vyle, J. S., Caruthers, M. H., and Cech, T. R. (1993) *Nature* 361, 85–88.
50. Weinstein, L. B., Jones, B., Cosstick, R., and Cech, T. R. (1997) *Nature* 388, 805–808.
51. Steitz, T. A., and Steitz, J. A. (1993) *Proc. Natl. Acad. Sci. U.S.A.* 90, 6498–6502.
52. Dahm, S. C., Derrick, W. B., and Uhlenbeck, O. C. (1993) *Biochemistry* 32, 13040–13045.
53. Nakano, S., and Bevilacqua, P. C. (2001) *J. Am. Chem. Soc.* 123, 11333–11334.
54. Nakano, S., Chadalavada, D. M., and Bevilacqua, P. C. (2000) *Science* 287, 1493–1497.
55. OrtolevaDonnelly, L., Kronman, M., and Strobel, S. A. (1998) *Biochemistry* 37, 12933–12942.
56. Yoshida, A., Sun, S. G., and Piccirilli, J. A. (1999) *Nat. Struct. Biol.* 6, 318–321.
57. Emerick, V. L., Pan, J., and Woodson, S. A. (1996) *Biochemistry* 35, 13469–13477.
58. Thibaudeau, C., and Chattopadhyaya, J. (1998) *Nucleosides Nucleotides* 17, 1589–1603.
59. Wilcox, D. E. (1996) *Chem. Rev.* 96, 2435–2458.
60. Steitz, T. A. (1998) *Nature* 391, 231–232.
61. Rosenberg, J. M. (1991) *Cur. Opin. Struct. Biol.* 1, 104–113.
62. Winkler, F. K. (1992) *Cur. Opin. Struct. Biol.* 2, 93–99.
63. Cooperman, B. (1976) in *Metal Ions in Biological Systems* (Sigel, H., Ed.) pp 79–125, Dekker, New York.
64. Benkovic, S., and Schray, K. J. (1978) in *Transition States of Biochemical Processes* (Gendour, R., Ed.) pp 493–527, Plenum, New York.
65. Herschlag, D., and Jencks, W. P. (1987) *J. Am. Chem. Soc.* 109, 4665–4674.
66. Herschlag, D., and Jencks, W. P. (1990) *Biochemistry* 29, 5172–5179.
67. Yarus, M. (1993) *FASEB J.* 7, 31–39.
68. Jencks, W. P. (1987) *Catalysis in Chemistry and Enzymology*, Dover Publications, New York.
69. Khan, K. S., and Kirby, A. J. (1970) *J. Chem. Soc. B*, 1172–1181.
70. Geyer, C. R., and Sen, D. (1997) *Chem. Biol.* 4, 579–593.
71. Nesbitt, S., Hegg, L. A., and Fedor, M. J. (1997) *Chem. Biol.* 4, 619–630.
72. Hampel, A., and Cowan, J. A. (1997) *Chem. Biol.* 4, 513–517.
73. Suga, H., Cowan, J. A., and Szostak, J. W. (1998) *Biochemistry* 37, 10118–10125.
74. Murray, J. B., Seyhan, A. A., Walter, N. G., Burke, J. M., and Scott, W. G. (1998) *Chem. Biol.* 5, 587–595.
75. Yoshida, A., Shan, S., Herschlag, D., and Piccirilli, J. A. (2000) *Chem. Biol.* 7, 85–96.
76. Ray, W. J., and Long, J. W. (1976) *Biochemistry* 15, 3993–4006.
77. Ray, W. J., Long, J. W., and Owens, J. D. (1976) *Biochemistry* 15, 4006–4017.
78. Carter, P., and Wells, J. A. (1988) *Nature* 332, 564–568.
79. Fersht, A. R., Knilljones, J. W., Bedouelle, H., and Winter, G. (1988) *Biochemistry* 27, 1581–1587.
80. First, E. A., and Fersht, A. R. (1995) *Biochemistry* 34, 5030–5043.
81. Leatherbarrow, R. J., Fersht, A. R., and Winter, G. (1985) *Proc. Natl. Acad. Sci. U.S.A.* 82, 7840–7844.
82. Wells, T. N. C., and Fersht, A. R. (1985) *Nature* 316, 656–657.
83. Whitty, A., Fierke, C. A., and Jencks, W. P. (1995) *Biochemistry* 34, 11678–11689.
84. Fierke, C. A., and Jencks, W. P. (1986) *J. Biol. Chem.* 261, 7603–7606.

BI0202631